Simulation Modelling Practice and Theory 19 (2011) 969–985

Contents lists available at ScienceDirect

Simulation Modelling Practice and Theory

journal homepage: www.elsevier.com/locate/simpat

A cellular automata model for circular movements of pedestrians during Tawaf

Siamak Sarmady [a,*], Fazilah Haron [a,b], Abdullah Zawawi Talib [a]

[a] School of Computer Sciences, Universiti Sains Malaysia, 11800 USM Penang, Malaysia
[b] Department of Computer Science, College of Computer Science and Engineering, Taibah University, P.O. Box 30002, Madinah, Saudi Arabia

ARTICLE INFO

Article history:
Received 16 October 2009
Received in revised form 8 November 2010
Accepted 7 December 2010
Available online 15 December 2010

Keywords:
Crowd simulation
Circular movements
Cellular automata
Discrete-event methods
Actions
Behaviours
Masjid Al-Haram
Tawaf

ABSTRACT

Masjid Al-Haram in Saudi Arabia is one of the most crowded pilgrimage locations in the world. More than two million pilgrims gather in Saudi Arabia annually during the Hajj season, and it is compulsory for them to perform a series of actions in the mosque. In the court area, pilgrims perform one of the most important rituals of Hajj, called Tawaf, which consists of seven laps of circular movement around the Kaabah, which is situated in the centre of the court. After the Tawaf, pilgrims pray in the court and leave from one of several doors. In this paper, we present a cellular automata model for the simulation of the pilgrims' circular Tawaf movement. We also use a discrete-event model to simulate the actions and behaviours of the pilgrims. The proposed models are used in a software platform to simulate the actions and movements of pilgrims in the area. We then present an example application of the model in predicting whether specific changes to the architecture could increase the throughput of the system.

1. Introduction

The large crowd of pilgrims attending the Muslim Holy Mosque in Makkah during Hajj makes it one of the most significant and complicated existing crowd management challenges. Each section of the mosque can host up to several thousands of pilgrims at one time. During peak periods, such as Hajj, tens of thousands of pilgrims circle around the Kaabah, while some perform prayers in the main court. The management of this large event requires a better understanding of the dynamics and behaviour of the crowd. A simulation model could help authorities to increase the performance of the system and to avoid dangerous incidents [1] by modifying structures or applying optimised rules to crowd movements. Furthermore, evacuation models could help in planning for emergency situations and in the training of the managing staff.

Fig. 1 shows a sketch of the mosque plan. Two of the most important areas in the mosque are the main court (Tawaf area) and the area between Safa and Marwah. Two central activities happen in these areas of the mosque. Pilgrims perform a circular movement around the small 11 × 12 m building, which is called Kaabah, in the centre of the main court. This circumambulation is called Tawaf and is performed seven times in an anticlockwise direction. Most of the pilgrims start and end Tawaf from an area that starts in front of the Hajar Al-Aswad (Fig. 2). The other important activity is Saie, in which pilgrims walk between Safa and Marwah seven times (Fig. 1).

Several crowd simulation models are available for either the simulation of evacuation or the normal movements of the crowd. Furthermore a few commercial products have also been available for a while. However based on our studies [2], these

* Corresponding author. Tel.: +60 17 4179800.
E-mail addresses: sarmady@cs.usm.my (S. Sarmady), fazilah@cs.usm.my (F. Haron), azht@cs.usm.my (A.Z. Talib).

1569-190X/$ - see front matter © 2010 Elsevier B.V. All rights reserved.
doi:10.1016/j.simpat.2010.12.004

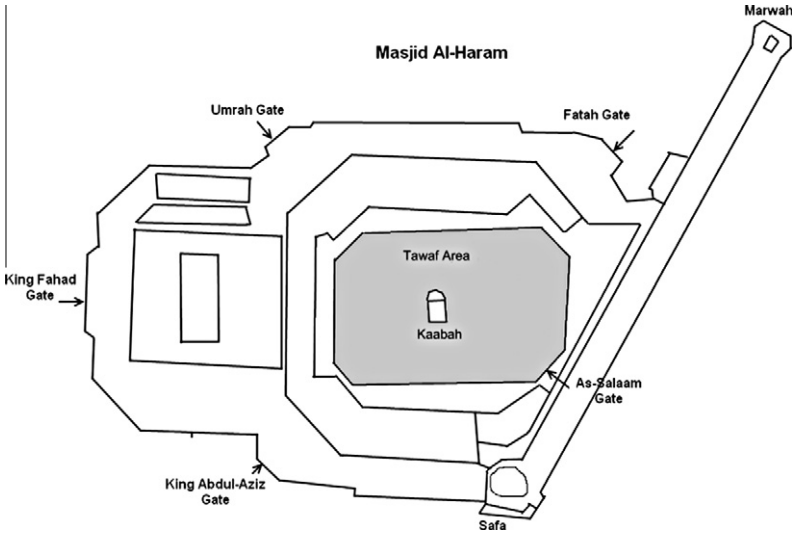

Fig. 1. A sketch of the Holy Mosque (Masjid Al-Haram).

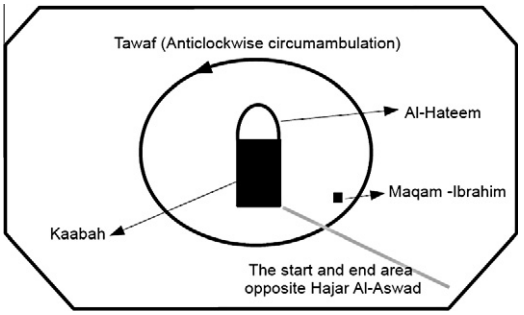

Fig. 2. The Tawaf area.

software are not able to simulate circular movements in Tawaf area with enough accuracy and details. Besides, these software normally can handle relatively small crowds. The huge crowd of up to 32,000 pilgrims in the court area cannot easily be simulated using the available software. The circular model we have proposed and implemented is able to simulate very large crowd of hundreds of thousands of pedestrians on a single personal computer with considerable amount of details.

In this paper, we focus mostly on the main court of the mosque and, specifically, the Tawaf movement. We present a basic framework for the actions and movements of pedestrians carrying out the Tawaf movement. We use a statistical discrete-event approach to simulate the pedestrians' actions, and use a model based on cellular automata to simulate their movements. We use two separate cellular automata models. One of them is specific to circular movements and the other simulates free walks between a source and a destination point. The simulation of actions and movements of individual pedestrians gives us insight into the emergent behaviours of the crowd. In this work we have proposed a circular cellular automata model which includes new rules, higher accuracy and flexibility compared to the existing models. The model also considers the details of Tawaf movement and integrates a discrete-event actions model into the crowd simulation. A crowd simulation architecture has also been created which is able to simulate very large crowds.

The organisation of the paper is as follows: Section 2 reviews the existing related work on crowd modelling and simulation. The social forces model, cellular automata models and rule-based model are discussed. In Section 3, we first suggest a basic layered model of the process of movement and then apply the different layers of the model to our simulation plan. We also discuss the relation of the proposed model to movements within the Tawaf area. In Section 4, we briefly present the architecture of the agent-based simulation platform created for this project. Finally, our conclusions are given in Section 5.

2. Related work

Various methods of modelling crowd movements have been used and reported in the literature. Physics-based models like particle and fluid dynamics models [3], force-based methods [4–9], matrix-based models [10–20] and, finally, rule-based models [21,22] are among the most commonly used methods. Fluid, gas dynamics and force-based approaches use physical

models to simulate movements. Matrix-based systems, on the other hand, divide environments into cells and make use of cellular automata to model the movements of entities between the cells. In rule-based models, simple creatures like birds, fishes and animals are simulated in the form of a flock and interact based on their perceptions of the environment.

Each of the models mentioned has its own weaknesses and advantages. Based on the specific requirements and simulation scenario, one model can be more suitable than the others. The social forces model, for example, produces smoother movements in comparison to cell-based methods due to its continuous nature. However, due to the computational complexity of the model, simulations based on it require a high processing power. In a sample study, Quinn et al. [23] used 11 CPUs to simulate the movements of 10,000 agents. For a large crowds like the one in the court of Masjid Al-Haram which can reach to over 32,000 pilgrims, it is not practical to use this method unless we incorporate a parallel processing technique. Moreover, simulations that result from this model appear like movements of particles rather than people, and at close distances, shaking effects are observed [24]. Pelechano et al. have created a modified model (HiDAC) by introducing braking and repulsion forces to avoid these unrealistic effects. Their model is also able to simulate the pushing, falling and trampling of pedestrians in a dense crowd. The HiDAC model has been used to simulate relatively small crowds of a few thousand individuals at a time [25].

Due to the cell structure of matrix-based models, movements of individuals between cells are not realistic. In addition, an individual's speed can only have a discrete value (such as 1, 2 or 3 cells in a simulation step). These limitations make such models unsuitable for applications that need smooth movements, such as animation production. However, the accuracy provided by these models might be sufficient to model emergent behaviours of a crowd. The simplicity of their transition rules makes these models very fast and allows them to be used for very large crowds. Modification of the rules and integration of the model into multi-layered behavioural simulations are also quite easy with such models. Rule-based methods, on the other hand, are more suitable for low-density crowds, and they can be used to build continuous models that provide smooth movements. However, these models use waiting rules and collision avoidance. Hence, they are not suitable for simulating dense crowds and panic situations in which collisions happen most of the time [26,27].

In real life, people move toward different goals and perform different actions in their environment. A lack of a model for goals and actions will result in a less realistic and comprehensive simulation. For this reason, behavioural models have recently been used on top of the movement models to achieve better simulations. Pelechano et al. [28], for example, integrated into their crowd simulation system an additional PMFserv human behaviour model that can influence the decision-making of agents at the microscopic and macroscopic movement levels in order to allow for more individualistic behaviour and therefore more realistic crowd simulation. In the PMFserv model, decision-making occurs based on emotion, stress level and physiology. In [29], McKenzie et al. built a cognitive human model that can be used for military simulations and general applications such as crowd simulation. In [30], Musse and Thalmann described their hierarchical model for simulating human crowds. In their work, they proposed a hierarchy that includes virtual crowds, groups and individuals. They provided three methods for controlling individual pedestrians including: innate and scripted behaviours, behavioural rules and external control in real time.

A few studies have been published on the court area of the mosque at Masjid Al-Haram. Al-Haboubi et al. [31] proposed a spiral movement path in the Tawaf area to decrease congestion and hence increase the throughput and the safety of the system. In [32], a microscopic simulation model for circular movements in the court area of the mosque was proposed. In this work, a non-uniform grid of cells is used to model the movements of individuals. The Tawaf area is divided into rings, and each ring is divided into equal-sized cells. The cell sizes in different rings are different; however, the area of each cell is almost equal. Simulation results are given for three different crowd-demand (entry) levels in the Tawaf area, including average speeds and the effect of different ratios of entries from four main doors on congestion and density. Koshak and Fouda [33] gathered empirical data from the Tawaf environment using GPS. In this experiment, the position and the speed of a circling pilgrim were recorded in ten trials on the three most congested days of the Hajj ritual. However, in this study, the low volume of data and the random movement paths make it difficult to calibrate a simulation. More accurate data on the average speeds in different positions, or points, in the Tawaf area, along with data on the status of the system during data gathering (number of pilgrims present, crowd densities and rate of entry into the area) would be useful for this purpose.

3. Models

Creating a model that covers all or most human behaviours could be very challenging and difficult. However, in a crowd, individuals perform more limited actions. In addition, the behaviours and actions that affect the emergent behaviour of the crowd are a small subset of all possible human behaviours and actions. Therefore, we have proposed a relatively simple and basic model that mostly focuses on human movements (Fig. 3). In [5], Helbing and Molnar discussed a similar model that takes stimuli, psychological/mental processes and actions into account when constructing crowd behaviour.

Typically, human movements start as a result of specific intentions and decisions. For example, after a person decides to visit a museum, he will perform a series of actions. These actions could include going to a train station, buying a ticket, travelling on a train and so on. Going to a train station is considered as a large-scale or macroscopic movement, which includes navigation and way-finding behaviours. To perform the macroscopic movements, microscopic local movements such as collision avoidance and shortest path selection take place. During these movements, environmental events and parameters may also trigger new decisions and actions. Consider an agent who intends to go into a room and exit through another door. From

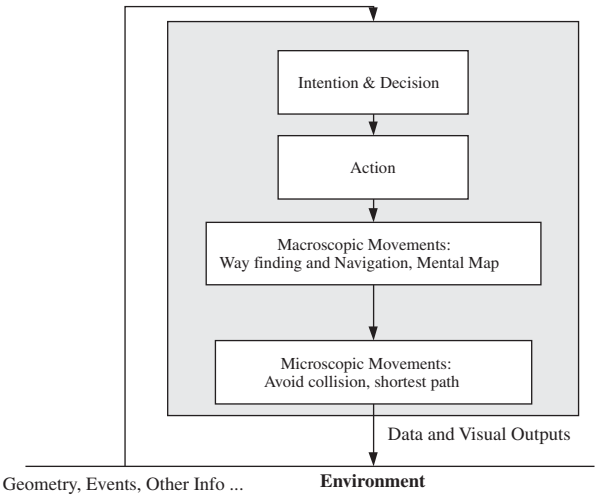

Fig. 3. Basic movement process model.

a macroscopic point of view, the agent should go from an entrance point to an exit point. From a microscopic point of view, however, agents exhibit very different and complex behaviours during the transition from one point to the other. Other agents, obstacles and walls may affect the agents' "shortest path selection" behaviour. Agents may need to make small changes to their paths: for example, stopping before reaching the next point.

Basic crowd models such as Helbing's social forces model [5] or the cellular automata model of Schadschneider [34] do not include a general model for individual actions. In this work, we attempt to create a more realistic simulation of the crowd by considering all of these concepts (intention and decision, action, macroscopic movements and microscopic movements).

3.1. Action model

The two higher layers in our basic four-layer model (Fig. 3) for human movement processes simulate intentions and actions. With actions and intentions limited to a specific set, it is possible to add discrete-event simulation methods to this framework to simulate the actions of individuals in a large crowd. We use the available data gathered from the Tawaf area in [35] and a few other resources to create the discrete-event model. Several rules (which exist in the real world) are applied to different layers of the model to reproduce a reasonable simulation of the Tawaf scenario. After achieving a nearly acceptable simulation, a larger and more accurate volume of data can be used to calibrate the system.

In the discrete-event method, a system or phenomenon is modelled as a sequence of events happening at specific points in time. In our case, each intention results in a sequence of actions. For example, people visit the Tawaf area of Masjid Al-Haram for different reasons. Some pilgrims go to pray in front of the Kaabah only while others carry out their pilgrimage actions like Tawaf, praying, Saie, etc. The selection of intentions—which will respectively map into sequences of actions—for each pilgrim will be done based on a random draw from available intention entries. The probability for each intention item will come from the empirical data. Table 1 shows an example series of intention template entries for the Tawaf scenario. Templates could change for different seasons and periods of the year.

The design of the action layer needs to be flexible in order to cover any combination of actions that a pilgrim might perform. In order to reproduce action series for individuals, we first create "action sequence templates". Each template is then assigned to an intention entry. During the simulation, templates are used to create series of actions for individual pilgrims. Therefore, it is necessary to define templates that cover action sequences that the majority of pilgrims might perform. In large crowds, especially when people perform similar series of actions (as do the pilgrims in our case), the actions of the majority of individuals can be covered by a small number of templates. Table 2 shows an example action sequence template.

The probability for each entry is used during the run time to identify whether the entry will be used for the list of actions of an individual pedestrian. Besides "Selection" and "Blocks", different actions (e.g., wait, pray, go) may have optional or

Table 1
Example intention entries and the sequence of actions mapped to them.

Intention (template)	Possible sequence of actions	Probability
Pilgrim intention – A	Enter from a door, Do Tawaf, Pray in front of Kaabah, Do Saie, Pray, Rest, Leave	0.33
Pilgrim intention – B	Enter from a door, Do Tawaf, Pray in front of Kaabah, Leave	0.11
Pilgrim intention – C	Enter from a door, Do Saie, Pray in front of Kaabah, Leave	0.12
Prayer intention - A	Enter from a door, Wait for prayer time, Pray in front of Kaabah, Leave	0.12

Table 2
An example action sequence template.

Probability	Action			P.1	P.2	P.3	P.4
1.0	Selection						
0.45		Enter		Gate-Abdulaziz			
0.14		Enter		Gate-Assalam			
0.11		Enter		Gate-Fahad			
0.04		Enter		Gate-Umrah			
0.04		Enter		Gate-Alfath			
0.22		Enter		Gate-Others			
1.0	Selection						
0.6		Block					
1.0			Go	Prayer area 1		Static	Least-Effort
1.0			Pray	480	100		
1.0			Go	Lower area		Static	Least-Effort
1.0			Wait	Exponential	200		
0.4		Block					
1.0			Go	Prayer area 1		Static	Least-Effort
1.0			Pray	480	100		
1.0			Go	Lower area		Static	Least-Effort
1.0	Selection						
0.53		Go		Gate-Abdulaziz		Static	Least-Effort
0.07		Go		Gate-Assalam		Static	Least-Effort
0.12		Go		Gate-Fahad		Static	Least-Effort
0.28		Go		Gate-Umrah		Static	Least-Effort
1.0	Exit						

Table 3
A concrete instance of an action sequence generated for a single pedestrian.

Action	P1	P2	P3	P4
Enter	Gate-Abdulaziz			
Go	Prayer area 1		Static	Least-Effort
Pray	495			
Go	Lower area		Static	Least-Effort
Go	Gate-Fahad		Static	Least-Effort
Exit				

compulsory parameters (P1–P4). The ''Go'' action, for example, needs a target for its first parameter, while the third and fourth parameters are used to identify the microscopic and macroscopic movement models being used for the ''Go'' action. Simple static path tables and least-effort models are used in this example. The template might also use blocks of actions and selections. During the run, the above template might result in the action sequence shown in Table 3 for a specific pedestrian.

Pedestrians are added to the simulation using a ''Demand Generator Function''. A Poisson distribution is used for this function. However, it is possible to use a different distribution for this purpose if the empirical data matches another distribution. In our simulation platform, it is possible to create a schedule that specifies different averages for different periods of the simulation, such as different times of the day.

The simulation of the next two layers of the four-layer model (i.e., those related to movements) requires us to model macroscopic way-finding and microscopic small-scale movements. To simulate movements in the entire Tawaf area or other parts of the mosque, we should navigate the pilgrims between different regions, and for the Tawaf, we will simulate the circular motion around Kaabah. The following sections will discuss the large-scale navigational and small-scale movements of individuals.

3.2. Way-finding and navigation model

Navigation between rooms and areas in a simulated environment is done in the macroscopic movement layer of our basic movement process model. For these sorts of large-scale movement decisions, different approaches have been used. A database of way-finding information—such as paths and routes from target to destination places—has been used in simulations previously [36]. This method is easy to implement and very fast; however, more complex models are also available. Knowledge about the location, communication between pedestrians and leader–follower behaviour is used in such models [28,27].

In a crowded place, finding the way is easier because even small numbers of pedestrians who know the environment, help others to find their way quickly [28,27]. Based on this assumption, in the simulation of large crowds, we can safely use a static path-finding table, which is easy to implement and very fast. We assume there are limited numbers of logical and suitable paths between every source and destination place. Shorter and better routes are given a lower cost in the path table. Table 4

Table 4
An Example of Way-finding Path Table Concept.

Source	Destination	Cost	MidP-1	MidP-2	MidP-3	MidP-4	MidP-5	MidP-6
Gate1	Gate2	1	–	-	–	–	–	–
Gate1	Gate6	2	Room1	-	–	–	–	–
Room4	Room7	3	Room3	Room5	–	–	–	–
...	...	...	...	...	...	...	...	...

shows the "Way-finding table" concept. Third entry in the table suggests a path between Room 4 and Room 7. This path needs the pedestrian to go through two inter-mediatory points. The cost assigned to this path is 3. Paths are then grouped by their cost and one of the paths are selected using a Poisson random number ($\lambda \ll 1$) in such a way that better routes are selected most of the time. It is possible to integrate parameters such as knowledge level, intelligence and stress level, taken from the behaviour level model (which simulates pedestrian behaviours) in the selection of paths. In our simulation, we just consider a few of the better routes for each source and destination point which have similar cost in most cases.

As for the circular Tawaf movement, large-scale navigation around the Kaabah is integrated in the microscopic movements layer in the form of maintaining a circular path around the Kaabah. However when the pedestrian tries to move from the Tawaf area to the prayer area or the doors, the way-finding layer will be used again.

3.3. Circular movement model

As mentioned before, Tawaf movement is basically a circular movement around the Kaabah building. The main idea behind the cellular automata model we have proposed in this section is that pilgrims maintain a circular path—or more accurately, a spiral—around the Kaabah. For other movements in the Tawaf area, such as moving from the Tawaf area toward the gates, we use a least-effort movement algorithm, which is a separate model. A higher layer of navigational behaviours is used to combine different types of movements (i.e., least-effort and circular) in order to simulate all of the movements of a pilgrim inside the main court of Masjid Al-Haram. In an earlier paper, we compared different available models for small-scale movements—such as force-based, cellular automata and rule-based models—and concluded that, because of the large number of crowd members in Masjid Al-Haram, a cellular automata model can result in faster simulations. We also noted that models such as social forces require parallel computation methods in order to simulate results in an acceptable time frame [37]. In this work, therefore, we use cellular automata for small-scale movements. We use agents to represent individuals. Each agent uses its perception and decision methods to select one of the eight Moore neighbours of the current cell for its next move (Fig. 4).

For the purpose of selecting the next cell, we first determine the desirability of each of the eight neighbouring cells (Fig. 5). The cell that has the least deviation from the individual's desired Tawaf radius and that, at the same time, is on the anticlockwise side of the current position is assigned the highest probability, and the cell that has the highest deviation from the desired radius and, at the same time, is on the clockwise side of the current position (i.e., the reverse direction of Tawaf movement) receives the lowest probability. In addition, if the cell is out of the grid or occupied by an object or another agent, a probability of zero will be assigned to it. In this way, crowd members will not only maintain a circular path, but will also move in an anticlockwise direction. In reality, however, pilgrims do not always follow a predetermined path, such as a specific radius from the centre of the circle, or maintain an anticlockwise direction. The probability-based model allows the agent to move into less desirable cells from time to time.

We use some of the ideas and conventions (e.g., parameter names) employed in [13,17] in our transition probability equation. These studies present a cellular automata model for the evacuation of an area. The model proposes equations that determine the probability of moving into each of the neighbouring cellular automata grid cells. Way-finding and local movements are integrated into a single model and use ant-like virtual traces left by individuals to orient other pedestrians. As described earlier, our navigational behaviours are taken care of in a separate "macroscopic movement" layer.

In the model, the transition probability P_i (the probability of moving into cell i) is given by:

$$P_i = N M_i \tag{1}$$

M_i is calculated for each of the neighbouring cells:

$$M_i = (1 - n_i)(1 - C m_i) e^{\beta \frac{D_{\min}}{D_i}} \tag{2}$$

$$D_{\min} = \mathrm{Min}(D_i), \quad n, m \in \{0, 1\}, \;\; 0 < C \leqslant 1, \;\; \beta \gg 0, \;\; D_i \neq 0$$

N is used to normalise the sum of probabilities of all eight cells to 1.

$$N = \frac{1}{\sum M_i} \tag{3}$$

As described earlier, the idea behind the model is that neighbouring cells with higher desirability and therefore higher probabilities will be selected most of the time. In the above equations, D_i is the deviation of cell i from the desired circumambulation radius. $D_{\min}$ is the deviation of the Moore neighbour nearest to the desired circular path (i.e., with the desired

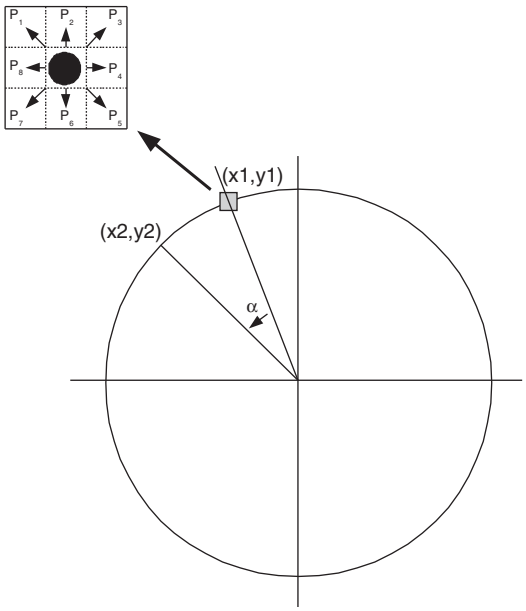

Fig. 4. Cellular automata next-cell selection in circular movement.

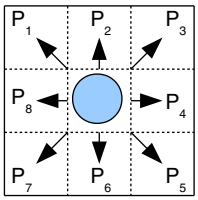

Fig. 5. Probabilities of moving into each of the eight Moore neighbouring cells.

radius). $D_{\min}/D_i$ specifies the ratio of the deviation of a specific cell in comparison to the cell with the least deviation. The difference between deviation values in Moore cells can be very small, and therefore, the probabilities of moving into each of the eight neighbouring cells may be very similar. We prefer the pedestrian to select the cell with the least deviation most of the time. In order to control the sharpness of the probability around the best cell, we use an exponential function. The β parameter in the exponent will fulfil our purpose. n_i identifies whether the ith cell is occupied by an individual. If a cell is already occupied, then n_i will be 1, which will cause the probability of moving into the occupied cells to become zero, thus providing collision avoidance. m_i determines whether the cell is on the anticlockwise side of the previous position. We could use a $(1 - m_i)$ term in our equation to completely filter any movement in the reverse direction of the Tawaf area, but it would be beneficial if we allowed a very small number of individuals to try cells in the reverse direction. These rare movements sometimes provide the chance of finding an empty position and leaving a congested area in case all anticlockwise cells are occupied. We have used a $(1 - Cm_i)$ term instead of $(1 - m_i)$ to introduce this option. C is a number very near or equal to 1 $(0 < C \leqslant 1)$.

An exception to the above equations occurs when one of the cells is located exactly at the desired radius from the Tawaf centre. In this case, if the cell is not occupied, the probability of moving into that cell will become 1 and every other cell will receive a probability of 0. Also, in extreme conditions $(\beta \to \infty)$, our equation will always result in the selection of the cell with the least deviation from the desired Tawaf movement radius:

$$P_i = \begin{cases} 1 & D_i = D_{\min} \\ 0 & \text{else} \end{cases} \tag{4}$$

In [13], Burstedde et al. suggested that their algorithm be run in two steps. In the first step, the next desired cell for each individual is identified. All of the movements happen in the subsequent step. If a target cell is already occupied, the individual will not move in that cycle. However, we use random movement turns for individuals in each cycle. We also use a density perception concept to control the speed of crowd members in relation to density. This concept will be discussed in Section 3.5.

3.4. Simplified circular CA algorithm

In the equation presented in the previous section, the use of large values for the β parameter might pose problems in calculating M_i as a result of a limited range of values in programming language variable types. In addition, the calculation of the relatively complex formula can be time-consuming. In order to solve the above-mentioned issues, we can use random numbers with desired distributions to select one of the cells for the next move. In this method, we first calculate M_i for each of the cells using the equation:

$$M_i = (1 - n_i)(1 - Cm_i)\frac{D_{\min}}{D_i} \tag{5}$$

$$D_{\min} = \mathrm{Min}(D_i), \qquad n, m \in \{0, 1\}, \quad 0 < C \leqslant 1, \quad D_i \neq 0$$

We then rank the cells based on their M_i value. The first index points to the cell with the least deviation from the desired circumambulation radius and should therefore be selected most of the time. Higher-indexed cells are selected less frequently. We then use a random number generator to select a cell from the possible moves based on either a predetermined probability vector or a specific distribution:

$$P = \begin{bmatrix} p_1 \\ p_2 \\ \cdots \\ p_8 \end{bmatrix} \tag{6}$$

$$\sum_{i=1}^{8} p_i = 1, \qquad 0 \leqslant p_i \leqslant 1 \tag{7}$$

In order to avoid the need for predetermined probability vectors and to provide more flexibility, it is possible to use a random number generator with Poisson distribution. It is easier to adjust the sharpness of the probability using the λ parameter rather than using several predefined probability vectors; therefore, we prefer this method. Different values for λ can be used for this purpose. Table 5 shows the probability of selecting each of the indexes with different λ values.

For the direct-line or least-effort movements of individuals inside the Tawaf area, we created a similar cellular automata model. This model uses the concept of least-effort [38] path selection as the basis of calculating the probabilities of moving into each of the neighbouring cells. The details of the least-effort movement model can be found in [39].

3.5. Modelling the effect of density on speed

In crowded areas, individuals tend to move more slowly than their free-flow speed in order to reduce the probability of a collision. In our direct-line and circular movement CA algorithms, however, crowd members move at their full free-flow speed until they reach another individual or an obstacle. The effect of density on speed has been studied by several researchers, mostly using empirically gathered data. Fig. 6 shows a graph by Fruin [40] that suggests that the speed of movements quickly drops as the density of pedestrians increases. In this graph, it is suggested that the movement speed reaches a very small value (close to zero) when the density approaches four pedestrians per square meter.

Based on this assumption, the equation below can be used to describe the density effect. By defining a higher margin for the effective density (ρ_0), we limit the slowdown in highly dense areas. In sparse areas, the speed decreases as the density increases, while in very dense areas (for example, denser than four individuals per square meter) the slowdown effect is restricted to avoid stalling movement.

$$DE = \begin{cases} \frac{\rho_{\text{path}}}{\rho_0}, & \rho_{\text{path}} < \rho_0 \\ 1, & \text{else} \end{cases} \tag{8}$$

We define the path as a small adjustable area toward the preferred direction (Fig. 7). This is equivalent to the perception of nearby obstacles by the pedestrian. Even though the shape of the area is not the same for corner and direct moves, the size

Table 5
Selection probability of cells with different standard deviation (σ) values.

Cell	$\lambda = 0.05$	$\lambda = 0.1$	$\lambda = 0.5$	$\lambda = 0.7$	$\lambda = 1.0$
1	0.951	0.904	0.607	0.496	0.367
2	0.047	0.090	0.302	0.348	0.367
3	0.001	0.004	0.076	0.122	0.183
4	0	0	0.012	0.028	0.061
5	0	0	0.001	0.004	0.015
6	0	0	0	0	0.003
7	0	0	0	0	0.0
8	0	0	0	0	0.0

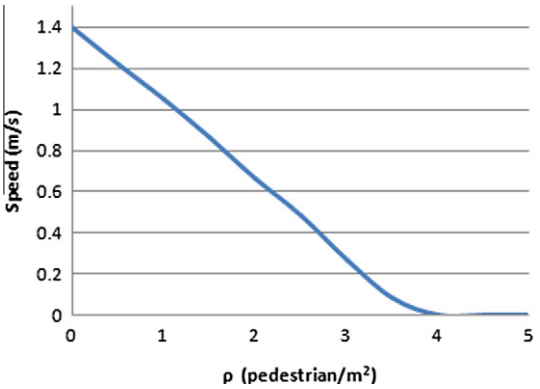

Fig. 6. Fruin's pedestrian speed–density relation graph [40].

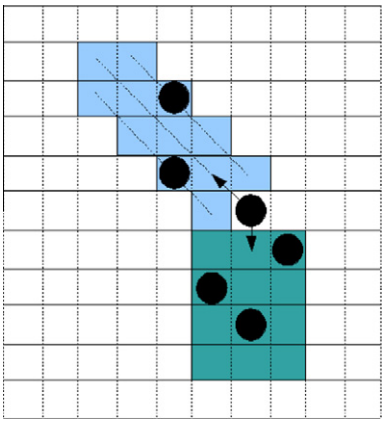

Fig. 7. Path area for direct and corner moves with a depth of four cells.

of each of the areas (12 cells in our example) is equal. In the above equation, ρ_{path} is the density of the path area and ρ_0 is the margin density.

Now we define a probability $P_{\text{Move–Stop}}$ such that, in low or zero densities, a pedestrian always perform its move. However, in higher densities, the pedestrian is prevented from moving in the current time step by the $P_{\text{Move–Stop}}$ probability:

$$P_{\text{move–stop}} = 1 - \mu(DE) \qquad 0 < \mu < 1 \tag{9}$$

In the above equation, μ is an adjustable parameter that allows us to control the overall effect of density on the probability of moving or stopping at each time step and thus its effect on crowd-member speed. The value of μ is adjusted by comparing the produced speed–density graph to the empirical graph derived from the empirical data or to other currently available speed–density graphs. The density margin ρ_0, the size of the path area (or its depth) and the value of μ are the parameters of our density effect model. It is also possible to generalise the density effect function to use any available density–speed function (or graph) other than the one used here.

$$DE = f(\text{density}) \tag{10}$$

3.6. Desired radius of pedestrians and size of the Tawaf circle

The radius of the circular crowd area is smaller when the number of pilgrims performing Tawaf is lower, and it increases as the number of pilgrims increases (Fig. 8). The maximum radius of the circle (around 48–50 m) is identified by the size of the Tawaf area, while the minimum radius is determined by the size of the Kaabah building (Fig. 9). The desired radius for each pilgrim is therefore randomly selected between these minimum and maximum radii.

We roughly estimate the size of the Tawaf circle in relation to the number of pilgrims using the graph presented in Fig. 10. The lower bound of the range is identified by considering the size of the Kaabah building itself (see Fig. 9). For the upper range, we have assumed that when the number of pilgrims passes a capacity margin, the entire area of the circle is used, and the size of the circle reaches its maximum. Based on the pictures of the Tawaf area, we estimate this margin to be around 3000–5000 pilgrims.

Fig. 8. Smaller number of pilgrims causes a smaller Tawaf circle.

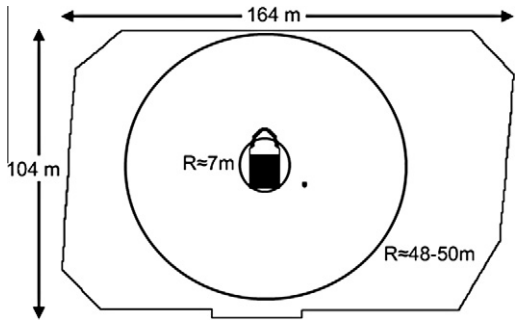

Fig. 9. Minimum and maximum size of the Tawaf circle.

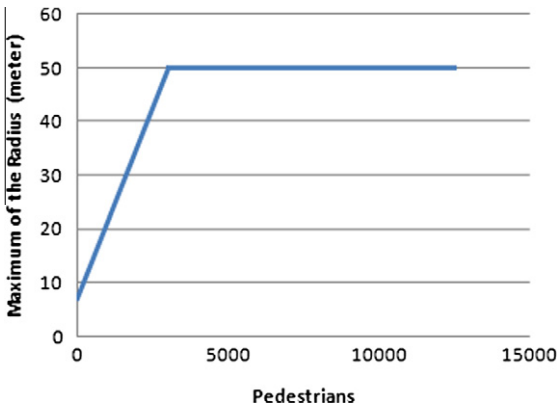

Fig. 10. An estimation of the relation between number of pilgrims and size of the Tawaf circle.

The maximum radius of the Tawaf circle at any moment is therefore:

$$\text{Max\_Radius} = \begin{cases} mN + R_{\min}, & N < \text{Margin\_capacity} \\ R_{\text{Max}}, & N \geqslant \text{Margin\_capacity} \end{cases} \tag{11}$$

$$M = \frac{R_{\max} - R_{\min}}{\text{Margin\_capacity}} \tag{12}$$

In this equation, $R_{\min}$ and $R_{\max}$ are the lower and higher bounds of the Tawaf circle (i.e., 7 m and 50 m). N is the number of pilgrims in the Tawaf area at the moment, and m is the slope of the graph line.

The use of a uniform distribution to generate a random radius between R_{Min} and R_{Max} for pilgrims will result in an excessive crowd density near the centre of the circle, because an equal number of individuals are assigned to both the smaller area near the Kaabah and the larger area farther from it. Instead, for the initial circumambulation radius for each pilgrim, we first use a uniform random process to find an unoccupied cell in the Tawaf circle area, considering the maximum Tawaf radius at any moment. We then use the distance of that free cell to the Tawaf centre as the initial circumambulation radius of the individual.

In this way, when the density of the crowd increases to excessive amounts in the areas near the Kaabah building, newly entering pilgrims will avoid choosing a radius near the building to avoid the very dense crowd—as would happen in reality. This is, however, an estimate, and a determination of the actual distribution requires sufficient empirical data and careful analysis.

As mentioned earlier, pilgrims tend to go gradually closer to the Kaabah (some even try to touch the Kaabah), creating a spiral trajectory. The amount of radius reduction in each time step is assumed to have a normal distribution for all pilgrims. The average reduction and standard deviation are adjustable parameters in the model.

3.7. Determining cell sizes, time step length and free-flow speed

Burstedde et al. [13] asserted that the velocity distribution of pedestrians is sharply peaked and that this fact leads to a model with a $V_{max} = 1$ cell in each time step, meaning that only transitions to neighbours are allowed. A greater maximum velocity would be difficult to implement in two dimensions due to the higher number of possible target cells and the need to check whether the path is blocked by other pedestrians; this makes the situation even more ambiguous for diagonal motion and crossing trajectories. In a dense crowd, the above assertion makes even more sense because crowd members are not free to move with whatever speed they want. They follow the crowd most of the time, and therefore, the maximum speed is mostly determined by the crowd. Individuals might want to move more slowly than the crowd, but again the crowd will somehow force them to adjust their speed to move with the crowd. We use a very similar approach. All crowd members (despite their differences) have the same minimum and maximum speed in our simulation, and individuals move either one cell at each time step or do not move at all.

The free-flow speed of pedestrians is the speed at which an individual will walk in the absence of any obstacle or other crowd members. The relation between density and speed in a crowd is shown in the form of speed–density graphs. Different average speeds and speed–density graphs have been suggested in which average speeds are between 1.0 m/s and 1.4 m/s. In [41], a list of possible reasons for the differences between the suggested fundamental speed–density graphs is given. These include cultural and population differences, differences between uni- and multidirectional flow, short-ranged fluctuations, the influence of psychological factors and the type of traffic (commuters, shoppers). In most cellular automata-based simulations such as the one used in [42], the average free-flow speed of crowd members is assumed to be 1.3 m/s. However, the walking speed of an individual is influenced by environmental parameters such as the temperature and humidity, as well as individual parameters like age, health, energy, fatigue and so on. Moreover, the free-flow speed decreases with time if the individual is walking a long distance. A good summary of these effects on the average speed of pedestrians has been studied in [43]. We do not have enough empirical data on the average walking speed of the people attending Tawaf. However, considering the length of the walk (between 30 min and sometimes more than 1 h) and the fact that 45% of the people attending Hajj are older than 46 years old (18% older than 55) [35], it is safe to consider a lower estimated free-flow speed of 1.1 m/s for the Tawaf area. Our simulation settings therefore produce an average speed of around 1.1 m/s in very low (close to zero) densities.

The cell size we have selected for this simulation is 40 cm $\times$ 40 cm, which matches most other cell-based simulations (such as [11,14,15,29,37,40,41]). The length of each simulation time step considered for the Tawaf simulation is 0.4 s.

3.8. Movement speed error

An important point to consider in the simulation is the difference between moving into the four corner Moore neighbour cells in comparison to the other four cells. Moving into corner cells displaces the individual about 0.56 m (considering a 0.4 $\times$ 0.4 cell size) while moving into direct cells will result into a 0.4 m displacement (Fig. 11). Within a similar number of cell transitions, an individual who moves mostly into corner cells will have a higher actual speed in comparison to a crowd member who moves into direct cells most of the time. Due to the discrete nature of the cellular automata and time steps, it is difficult to solve this problem completely. However, to make things better, we introduce a limit to the distance an individual can move in a specific time interval based on the maximum free-flow speed of a pedestrian. If an individual's next move exceeds the allowed distance one can move in 1 s, the movement will be prohibited.

Table 6 shows possible combinations of movements for three consecutive moves for cell sizes of 0.4 m $\times$ 0.4 m. In the case in which a pedestrian tries to move to a corner three times in a row, the last move will be avoided.

Without applying the cap, the difference between the maximum and minimum displacement (MaxMove and MinMove) in three consecutive moves will be:

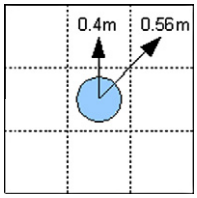

Fig. 11. Displacement of moving into the four corner cells and the other four cells.

Table 6
Actual displacement of pedestrian in three moves after applying the cap.

1st Move	2nd Move	3rd Move	Default displacement (m)	Actual displacement (m)
D	D	D	1.2	1.2
D	D	C	1.36	1.36
D	C	D	1.36	1.36
D	C	C	1.52	1.52
C	D	D	1.36	1.36
C	D	C	1.52	1.52
C	C	D	1.52	1.52
C	C	C	~~1.68~~	1.12

$$\text{Difference Error} = \frac{\text{MaxMove} - \text{MinMove}}{\text{MinMove}} = \frac{1.68 - 1.2}{1.2} \times 100 = 40\% \tag{13}$$

By applying a cap of 1.52 m in three time steps, we have a slightly lower error level:

$$\text{Difference Error} = \frac{1.52 - 1.12}{1.12} \times 100 = 35.71\% \tag{14}$$

Even though this method is used to minimise the error, it can introduce more error itself if the capping limit is not chosen correctly; therefore, we use a simple program that examines all possible moves and selects the best cap value to be applied to a specific number of moves. It can be shown that applying a cap at a higher number of moves produces better results. For the case study of the Tawaf area, we have cell sizes of 0.4 m × 0.4 m, and each time step is equal to 0.4 s. If we want to apply the cap every five moves, the best cap value will be 2.32 m (1.16 m/s). The errors for our cell size with and without the cap level will be:

$$\text{Difference Error} = \frac{2.8 - 2}{2} \times 100 = 40\% \tag{15}$$

$$\text{Difference Error with Cap} = \frac{2.32 - 1.92}{1.92} \times 100 = 20.83\% \tag{16}$$

4. Simulation platform architecture

The simulation platform consists of a simulation engine and a few supporting modules (Fig. 12). The simulation engine itself consists of two sub-modules. MiCS (Micro–macro Crowd Simulator module) is responsible for the physical movement of the crowd members while MABS (Multi-Agent Behaviour Simulator module) simulates their actions and behaviours.

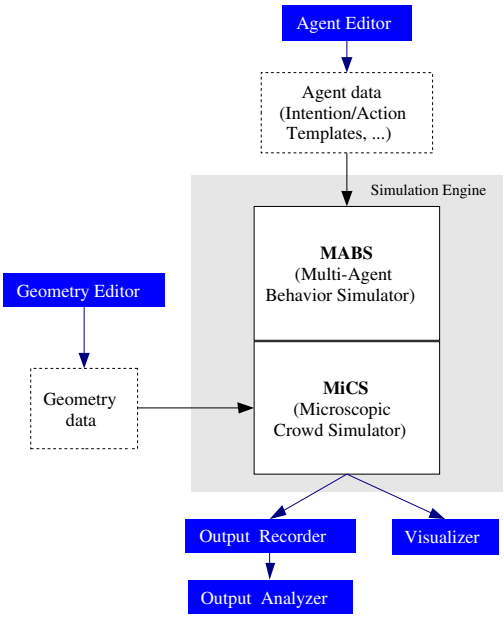

Fig. 12. Architecture of the software platform.

Agent Editor and Geometry Editor are modules that feed the system with pedestrian and geometry input data. The Visualiser module displays the results, while the Output Recorder and Output Analyser help to produce reports. The software was developed using Java SE 1.6. The resulting software proved that the proposed model is capable of simulating a very large crowd. In contrast to social forces implementations, which are limited to a few thousand pedestrians on a single computer, we were able to simulate around 22,000–23,000 agents in real time (1 s of simulation time using 1 s of computing time). Optimising the code and using more parallel techniques will allow for the simulation of even larger crowds using a single computer.

5. Simulation results

In this section, we first compare the speed–density graphs obtained from the simulation to the available graphs obtained from empirical observations. In addition, we compare simulation snapshots with photos taken at the actual place. We then present a graph showing the duration of Tawaf in relation to the demand level (hence the number of people doing Tawaf) and, finally, use the system to predict whether opening the Al-Hateem wall in the northern part of the Kaabah building would provide a meaningful increase in the system throughput.

5.1. Speed–density graph

In Section 3.8, we mentioned that different empirical speed–density graphs are available. Even though the graphs are different, the speed decreases when the density increases in all of them. We do not have any strong reason to select one of the available graphs over the others, and unfortunately, we are not aware of any empirical graphs for this mosque or for the Tawaf movement. Therefore, we compare our results with only two of the graphs listed in [41]. Fruin's and Predtechenskii–Milinskii's (PM) graphs can be considered as the extremes among the available graphs. Fruin's graph has the highest free-flow speed (1.4 m/s), while PM's graph shows the lowest (1.0 m/s). Fruin's graph suggests that a density of 4 pedestrians/m^2 will cause the crowd to stop, while PM's graph suggests that a crowd with a density of higher than 8 pedestrians/m^2 can continue moving with speeds of under 0.2 m/s. In places close to the Kaabah, where extreme densities of over 6 pedestrians/m^2 can sometimes be observed, pilgrims continue to move at slower speeds. As a result, we are inclined to conclude that the real speed–density graph for this mosque, the specific type of movement—moving as part of a ritual—and the crowd of pilgrims should be similar to that described in Predtechenskii and Milinskii's graph.

Different sections of the Tawaf area in the Masjid Al-Haram court have different properties. We have therefore divided the Tawaf circle into sub-sections in order to have separate speed–density graphs for each of them (Fig. 13). The Kaabah walls, especially those parts that are in section I4, are very attractive to pilgrims (simulated by attraction points), and they attempt to reach and touch the walls and pray near this section. Additionally, people normally move slower as they near the walls. In sections I4, M4 and O4, there is an arbitrary Tawaf start–finish line or area. People make a small delay in the area (simulated by delay marks) and then start their Tawaf or cross the Tawaf circumambulation to exit. We prefer the O1, O2, O3, M1, M2 and M3 areas for comparison because they lack such special features.

In Fig. 14, we have compared the speed–density graphs of the M1 and M2 areas to Fruin's (SPFE) and Predtechenskii and Milinskii's (PM) graphs. As can be observed, the graphs of these two areas follow the PM graph. However, the initial free-flow speed in the PM graph is around 1.0 m/s, while in our case, the free-flow speed is set at around 1.1 m/s. Considering the difference between our free-flow speed and that of the PM graph, it can be concluded that the speed-density graphs for M1 and

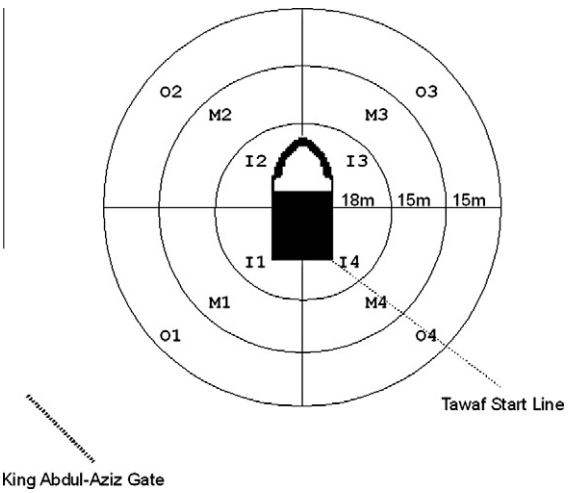

Fig. 13. Dividing the Tawaf circle into sub-areas for speed–density investigation.

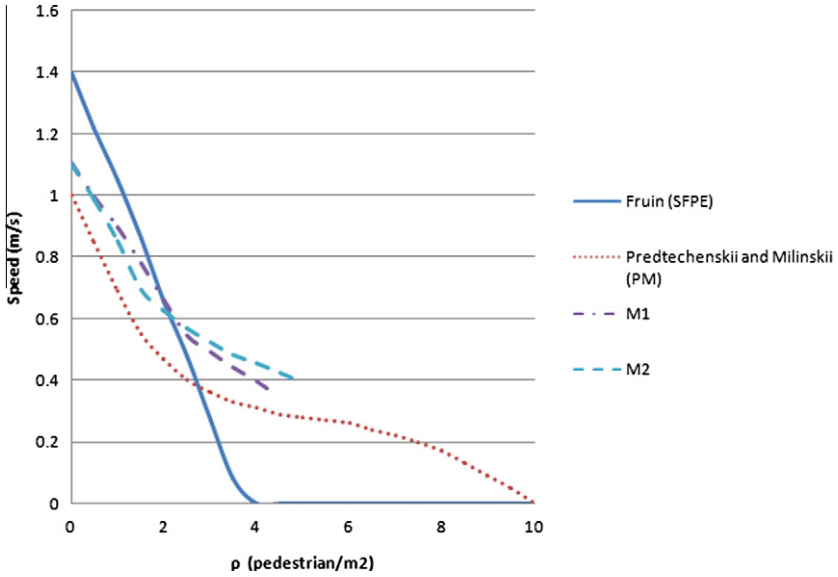

Fig. 14. Speed–density graphs for the M1 and M2 regions.

M2 are very similar to the fundamental PM graph. It should be mentioned that the maximum density in our cellular automata model is 6.25 pedestrians/m^2 (dictated by our cell size of 0.4 m $\times$ 0.4 m). In addition, even with very high demand levels, we could not reach densities higher than 5 pedestrians/m^2 in the M1 and M2 regions.

5.2. Visual comparison

As mentioned above, the Tawaf system has several features in its different areas. The "start–end line", attraction points such as Hajar Al-Aswad and Maqam-Ibrahim, the shape of the Kaabah, the semi-circular Al-Hateem wall on the north side of

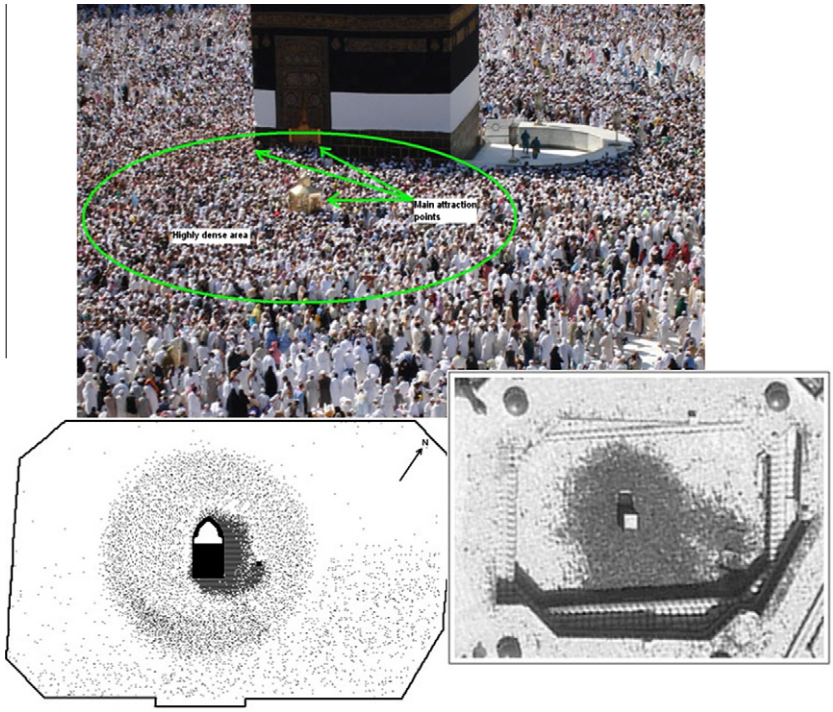

Fig. 15. Congested area in the east side of the Kaabah (top), simulation snapshot (bottom left) and satellite photo (bottom right).

the Kaabah and the shape of the Tawaf area have the most important roles in the system. The centre of the circumambulation of Tawaf is based on the visual perception of the pilgrims of the Kaabah building and the lines drawn on the floor. Pilgrims try to circle the Kaabah by maintaining a circular path around it (or spiral for some of the pedestrians). However, the Al-Hateem wall is an extension of the Kaabah, and it produces additional resistance against circular crowd flow. This resistance against the anticlockwise Tawaf motion creates a highly dense and congested area near Al-Hateem. This congestion, combined with the congestion created by the attractions on the east side of the Kaabah, causes a highly dense area in that side of the Kaabah, while the other side of the Kaabah is less congested. Fig. 15 shows a snapshot of the simulation at a medium demand level. As can be seen, the simulation has reproduced the congested area in the east side of the Kaabah as well as the gathering around Maqam-Ibrahim. On the right side of the court is a place where pilgrims pray, and in the lower section, they stand and sometimes rest. All of these details can also be seen in the simulation snapshot. The circular form of the crowd can also be observed in the satellite photo.

5.3. Tawaf duration and speed

A larger number of pilgrims in the Tawaf circle will result in a slower Tawaf motion. In Fig. 17, the simulation has been run for five different demand levels: 5000, 7500, 10,000, 12,500 and 15,000 pilgrims per hour. These levels reflect low, medium, high, very high and extremely high demand levels. We then calculated the average Tawaf time for the first 2000 pilgrims finishing their Tawaf action. It can be easily observed that the Tawaf average duration increases when the demand level increases. It can also be observed that demand levels higher than 10,000 pedestrians per hour cause a sharp increase in Tawaf time (Fig. 16). The simulation animation reveals that, at this demand level, congestion starts to develop behind the Tawaf start–end line. This congestion could spread to even larger areas in the Tawaf circle and cause longer and longer Tawaf durations. High congestion levels might become dangerous because people might push each other in such situations.

The average speeds of the Tawaf movement and the duration of Tawaf in our simulation match the ranges of speeds and duration given in Koshak and Fouda's work [33]. However, more data is required to more accurately calibrate the simulation parameters.

5.4. Example applications of the simulation

We have used the simulation of the Tawaf area to identify whether specific changes to the area or the operation rules would pose a considerable change to the throughput of the system. In one of the experiments, we opened the Al-Hateem wall (the semi-circular wall in the north of the Kaabah building) to the pilgrims during Tawaf. We should mention that this change might not be possible in reality due to the religious significance of the wall. Based on the results of our simulation, the opening of Al-Hateem would be expected to have a considerable effect on the throughput of the Tawaf system. This is because the removal of the Al-Hateem section would cause the shape of the object in the centre of the Tawaf, the Kaabah building, to be more similar to a square than to a rectangle. A square would generate less resistance to the circular movement of the crowd, and the minimum walking length needed to finish Tawaf would be shorter. The graph in Fig. 17 shows the results. The opening of the Al-Hateem area to Tawaf, according to our simulation (demand level: 7500 pedestrians per hour), would provide 1580 pedestrians or 17% more throughput in a 2-hour period.

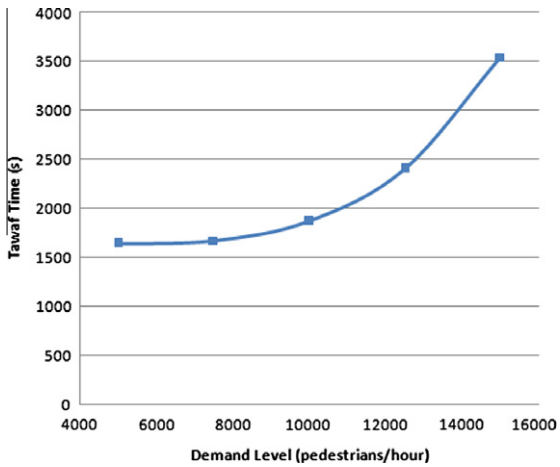

Fig. 16. Duration of Tawaf action in different demand levels.

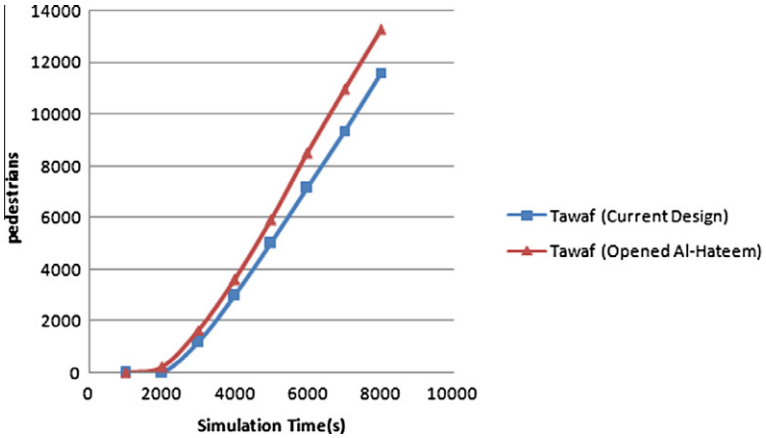

Fig. 17. Throughput in the current design and if the Al-Hateem area was open.

6. Conclusion

In this paper, we have presented an approach that we believe to be suitable for simulating large and dense crowds in the Tawaf area and other congested places. We presented a basic model for pedestrian movement processes and developed models for each of its layers. We used discrete-event methods to simulate the actions of individuals in a large crowd. We also used a cellular automata model to simulate their small-scale movements. A circular cellular automata model was devised to simulate the Tawaf movement. A crowd simulation platform was developed and used to study the crowd in the area. The software was used to predict whether changes to the area or to the operation of the place would create a significant gain in the throughput of the system. Future research will continue in two directions: creating a more accurate small-scale movement model that considers specific issues of dense crowds, such as pushing, falling and grouping of individuals, and a better model of crowd members that considers physiological, psychological and sociological aspects of human actions in order to produce more realistic simulations of crowds.

Acknowledgement

This research was partially supported by the USM-FRGS grant title "Computational Models for Human Movement and Behaviour: A case study of the Tawaf area" and USM PhD Fellowship.

References

[1] G.K. Still. Crowd disasters, July 2010. <http://www.gkstill.com/CrowdDisasters.html>.
[2] S. Sarmady, F. Haron, M.M.M. Salahudin, et al, Evaluation of existing software for simulating of crowd at Masjid Al-Haram, Jurnal Pengurusan Jabatan Wakaf Zakat & Haji 1 (1) (2007) 83–95.
[3] D. Helbing, A fluid-dynamic model for the movement of pedestrians, Complex Systems 6 (1992) 391–415.
[4] D. Helbing, I. Farakas, T. Vicsek, Simulating dynamical features of escape panic, Nature 407 (2000) 487–490.
[5] D. Helbing, P. Molnar, A social force model for pedestrian dynamics, Physical Review E 51 (1995) 4282–4286.
[6] D. Helbing, P. Molnar, I.J. Farkas, et al, Self-organizing pedestrian movement, Environment and Planning B: Planning and Design 28 (2001) 361–383.
[7] S. Okazaki, S. Matsushita, A study of simulation model for pedestrian movement with evacuation and queuing, in: Proceedings of International Conference on Engineering for Crowd Safety, 1993, pp. 271–280.
[8] S. Okazaki, Movement in architectural space. Part 1: Pedestrian movement by the application of magnetic models, Transactions of Architectural Institute of Japan (283) (1979) 111–119.
[9] K. Teknomo, Y. Takeyama, H. Inamura, Microscopic pedestrian simulation model to evaluate lane-like segregation of pedestrian crossing, in: Proceedings of Infrastructure Planning Conference, Japan, 2001, p. 208.
[10] V.J. Blue, J.L. Adler, Emergent fundamental pedestrian flows from cellular automata microsimulation, Transportation Research Record (1644) (1998) 29–36.
[11] V.J. Blue, J.L. Adler, Cellular automata micro-simulation of bi-directional pedestrian flows, Journal of the Transportation Research (2000) 135–141.
[12] V.J. Blue, J.L. Adler, Modeling four-directional pedestrian movements, in: 79th Annual Meeting of the Transportation Research Board, January 2000.
[13] C. Burstedde, K. Klauck, A. Schadschneider, et al, Simulation of pedestrian dynamics using a two dimensional cellular automation, Physica A 295 (2001) 507–525.
[14] J. Dijkstra, Towards a multi-agent model for visualizing simulated user behavior to support the assessment of design performance, in: Proceedings of Media and Design Process – ACADIA'99, Salt Lake City, USA, 1999, pp. 226–237.
[15] J. Dijkstra, A.J. Jessurun, A multi-agent cellular automata system for visualising simulated pedestrian activity, in: Proceedings on the 4th International Conference on Cellular Automata for Research and Industry, Karlsruhe, 2000, pp. 29–36.
[16] A. Kirchner, K. Nishinari, A. Schadschneider, Friction effects and clogging in a cellular automaton model for pedestrian dynamics, Physical Review E 67 (5) (2003) 056122.
[17] A. Schadschneider, A. Kirchner, K. Nishinari, CA approach to collective phenomena in pedestrian dynamics, in: Proceedings of the 5th International Conference on Cellular Automata for Research and Industry, 2002, pp. 239–248.

[18] P. Thompson, H. Lindstrom, P. Ohlsson, et al., Simulex: analysis and changes for IMO compliance, in: Proceedings of 2nd International Conference: Pedestrian and Evacuation Dynamics, 2003, pp. 173–184.
[19] T.J. Lightfoot, G. Milne, Modelling emergent crowd behaviour, in: Proceedings of the 1st Australian Conference on Artificial Life, Canberra, December 2003, pp. 159–169.
[20] H.L. Klüpfel, A Cellular Automaton Model for Crowd Movement and Egress Simulation, PhD thesis, University Duisburg-Essen, 2003.
[21] C. Reynolds, Flocks, herds, and schools: a distributed behavior model, in: Proceedings of ACM SIGGRAPH, 1987, pp. 25–34.
[22] C. Reynolds, Steering behaviors for autonomous characters, in: Proceedings of Game Developers Conference, San Jose, California, 1999, pp. 763–782.
[23] M. Quinn, R. Metoyer, K. Hunter-Zaworski, Parallel implementation of the social forces model, in: Proceedings of the Second International Conference in Pedestrian and Evacuation Dynamics, 2003, pp. 63–74.
[24] N. Pelechano, N. Badler, Improving the Realism of Agent Movement for High Density Crowd Simulation, University of Pennsylvania, Center for Human Modeling and Simulation, 2006.
[25] B.G. Silverman, M. Johns, J. Cornwell, et al, Human behavior models for agents in simulators and games. Part I: Enabling science with PMFserv, Presence 15 (2) (2006) 139–162.
[26] N. Pelechano, C. Stocker, J. Allbeck, et al., Being a part of the crowd: towards validating VR crowds using presence, in: Proceedings of the 7th International Joint Conference on Autonomous Agents and Multiagent Systems, vol. 1, Estoril, Portugal, 2008, pp. 136–142.
[27] N. Pelechano, N. Badler, Modeling crowd and trained leader behavior during building evacuation, IEEE Computer Graphics and Applications 26 (6) (2006) 80–86.
[28] N. Pelechano, K. O'Brien, B. Silverman, et al., Crowd simulation incorporating agent psychological models, roles and communication, in'' First International Workshop on Crowd Simulation, 2005, pp. 21–30.
[29] Q.H. Nguyen, F.D. McKenzie, M.D. Petty, Crowd behavior cognitive model architecture design, in: Conference on Behavior Representation in Modeling and Simulation, Orlando, 2005.
[30] M. Soraia Raupp, T. Daniel, Hierarchical model for real time simulation of virtual human crowds, IEEE Transactions on Visualization and Computer Graphics (7 2) (2001) 152–164.
[31] H. A.-H. Muhammad, Z.S. Shokri, A design to minimize congestion around the Ka'aba, Computers & Industrial Engineering 32 (2) (1997) 419–428.
[32] A. Abdelghany, K. Abdelghany, H.S. Mahmassani, et al, Microsimulation assignment model for multidirectional pedestrian movement in congested facilities, Transportation Research Record 1939 (2006) 123–132.
[33] N. Koshak, A.A.M. Fouda, Analyzing pedestrian movement in Tawaf using GPS and GIS, in: Proceedings of Map Asia, Beijing, China, 2004.
[34] A. Schadschneider, Cellular Automaton Approach to Pedestrian Dynamics – Theory, Pedestrian and Evacuation Dynamics, Springer, 2002. pp. 75–86.
[35] W.S. Halabi, Overcrowding and the Holy Mosque, Makkah, Saudi Arabia,'' PhD thesis, Dept. of Architecture, University of Newcastle upon Tyne, 2006.
[36] A. Kamphuis, M. Rook, M.H. Overmars, Tactical path finding in urban environments, in: Proceedings First International Workshop on Crowd Simulation, Lausanne, 2005, pp. 51–60.
[37] S. Sarmady, F. Haron, A.Z.H. Talib, Multi-agent simulation of circular pedestrian movements using cellular automata, in: Proceedings of 2008 Second Asia International Conference on Modelling & Simulation, Kuala Lumpur, Malaysia, 2008, pp. 654–659.
[38] G.K. Zipf, Human Behavior and the Principle of Least Effort, Addison-Wesley, Reading, Mass, 1949.
[39] S. Sarmady, F. Haron, A.Z.H. Talib, Modeling groups of pedestrians in least effort crowd movements using cellular automata, in: Proceedings of 2009 Second Asia International Conference on Modelling & Simulation, Bali, Indonesia, 2009, pp. 520–525.
[40] J.J. Fruin, Pedestrian Planning and Design, Metropolitan Association of Urban Designers and Environmental Planners, New York, 1971.
[41] A. Schadschneider, W. Klingsch, H. Klüpfel, et al, Modeling and applications, in: B. Meyers (Ed.), Encyclopedia of Complexity and System Science, Springer, Berlin, 2008.
[42] G.K. Still, Crowd dynamics, PhD thesis, University of Warwick, August 2000.
[43] R.L. Knoblauch, M.T. Pietrucha, M. Nitzburg, Field studies of pedestrian walking speed and start-up time, Transportation Research Record (1538) (1996) 27–38.